

Influence of frictional mechanism on chatter vibrations in the cutting process—analytical approach

Andrzej Weremczuk¹ · Rafal Rusinek¹ 

Received: 12 July 2016 / Accepted: 21 September 2016 / Published online: 7 October 2016
© The Author(s) 2016. This article is published with open access at Springerlink.com

Abstract The paper examines a nonlinear one-degree-of-freedom model of the cutting process. The classical regenerative mechanism of chatter is enriched by an additional friction phenomenon which generates frictional chatter. Additionally, the nonlinear cubic stiffness of the tool is taken into account. The aim of the paper is to investigate interactions between regeneration and the frictional effect. The proposed model is solved by the multi-time scale method. The cutting process stability (trivial solution) is determined in order to produce stability lobe diagrams and determine the influence of friction on the process. Finally, the maps of chatter amplitudes are presented and new frictional stability lobe diagrams are proposed to analyse the influence of friction.

Keywords Frictional chatter · Regenerative chatter · Cutting process

1 Introduction

Nowadays the cutting process is still one of the most popular manufacturing methods. Given increased industrial competition, the manufacturers must reduce costs and improve dimensional accuracy. The efficiency of a machining operation is determined by the metal removal rates, cycle time, machine down time and tool wear. The primary factor

that limits machining process efficiency is a phenomenon called chatter. Chatter is a dynamic instability that can limit material removal rates, cause poor surface finish and even damage the tool or the workpiece. From a historical point of view, the knowledge of machine tool chatter goes back to almost 100 years ago when Taylor first described this phenomenon [1]. Next, Tlustý et al. [2], Tobias [3] and Kudinov [4, 5] gave background of the so-called regenerative chatter. This effect has become the most commonly accepted explanation for machine tool chatter. Later, however, another chatter mechanism produced by friction was developed by Grabec [6]. This mechanism, called frictional chatter, can cause interesting phenomena such as deterministic chaos [6–11]. While the frictional mechanism is based on friction between the tool and the workpiece, the regenerative effect is related to the wavy workpiece surface generated by the previous cutting tooth pass. Wiercigroch et al. define four chatter mechanisms [12, 13]. Besides regenerative and frictional chatter, they also report mode coupling and thermo-mechanical mechanisms. Although trace regeneration and friction are very important practical operations, there are few papers which consider regenerative and frictional mechanisms together, for example [14]. Since friction always exists in a real cutting process, excluding this phenomenon would be a too big simplification.

In the literature, the most often discussed operations are orthogonal cutting operations, e.g. turning and milling. As for turning, the governing equation is relatively simple because the tool has one cutting tooth which still is in contact with the workpiece, so the depth of cut is positive [12, 13, 15, 16]. In the case of milling, the direction and value of the cutting force change due to rotation of the multi-blade tool, and the cutting is interrupted as each tooth enters and leaves the workpiece. Consequently, the resulting equation of motion is non-smooth [17, 18]. This causes problems

✉ Rafal Rusinek
r.rusinek@pollub.pl
Andrzej Weremczuk
a.weremczuk@pollub.pl

¹ Lublin University of Technology, Nadbystrzycka 36,
20-618 Lublin, Poland

during numerical and analytical calculations. An analytical solution of nonlinear problems is not exact but approximate and difficult to obtain. Nonetheless, it is frequently used due to its universality [19]. Sometimes, the impact of ploughing mechanism on chatter stability is presented as well [20].

Recently, scientists pay attention on dynamics of cutting process where multifunctional tools [21] and tools for special operations e.g. thread milling [22] are used. Moreover, the problem of stability lobes in milling process with multiple modes is analysed [23]. In this paper, the useful method of the lowest envelop stability lobes is developed.

In order to get knowledge about the influence of frictional chatter on regenerative chatter and complete field of mathematical approach, the method of time multi-scales is applied here. An explanation of interactions between the frictional and regenerative mechanisms is the main aim of the paper. Therefore, the dynamics of a one-degree-of-freedom model of the cutting process is examined. Special attention is devoted to the stability problem of trivial and non-trivial solutions and their dependence on system parameters. Finally, some practical conclusions regarding the cutting process are drawn from the results.

2 Mathematical model

For the purpose of analysing the regenerative and frictional mechanisms of chatter, a one-degree-of-freedom model of orthogonal cutting is presented in Fig. 1. In order to explain interactions between the regenerative and frictional mechanisms, only the feed direction (x) is considered here. From our point of view, the feed direction is more important, particularly because the regenerative mechanism depends on tool position in the x (feed) direction and friction between the tool and the chip. The tool is modelled as a lumped mass which is suspended with a nonlinear spring and a linear (viscous) damper. The nonlinear spring is sometimes used in the literature (e.g. [19, 24]) to model the nonlinear properties of the tool and tool holder, although a linear spring

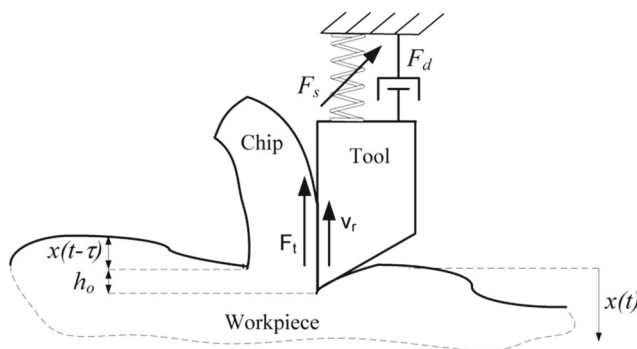


Fig. 1 Model of orthogonal cutting

is more popular. The differential equation of tool motion is presented as

$$m\ddot{x}_1(t) + c\dot{x}_1(t) + k_1x_1^3(t) + kx_1(t) = K_r w \cdot (h_o - x_1(t) + x_1(t - \tau)) + K_t(\text{sgn}(v_r) - a_r v_r + b_r v_r^3) \tag{1}$$

where, m is the tool mass, c is damping, k and k_1 are the linear and nonlinear stiffness coefficients, w is the width of cut, and h_o is the initial depth of cut. K_r is the regenerative component of the specific cutting force which is related to material shearing (regenerative effect), while K_t is the frictional component of the specific cutting force. Dividing Eq. 1 by m and introducing the non-dimensional coordinate (x) and time, after some calculations the non-dimensional spring and damping forces (F_s and F_d) are expressed as

$$F_s = \gamma x^3(t) + \omega_0^2 x(t) \\ F_d = \delta \dot{x}(t) \tag{2}$$

The delay differential equation of motion can be presented in a non-dimensional form as

$$\ddot{x}(t) + \delta \dot{x}(t) + \gamma x^3(t) + \omega_0^2 x(t) \\ = \alpha(h_o - x(t) + x(t - \tau)) + \beta(\text{sgn}(v_r) - a_r v_r + b_r v_r^3) \tag{3}$$

Despite the fact that the regenerative effect is the main cause of chatter, one cannot neglect friction phenomena between the tool and the workpiece as well as between the chip and the tool. Therefore, the present model of the cutting force has two components. A regenerative force, which occurs when the favourable phase develops between the inner and outer modulations, and a friction force between the tool and the workpiece. Then, α denotes the cutting resistance of the regenerative force (regenerative force factor) while β is the cutting resistance of the friction force component (friction force factor). In other words, α and β tell us how strong the regenerative and the friction components are. The regenerative force depends on the depth of cut (h_o), the present tool position $x(t)$ and the previous position $x(t - \tau)$. In turn, the time delay $x(\tau)$ is connected with the spindle speed Ω by the equation

$$\Omega = \frac{2\pi}{\tau} \tag{4}$$

The friction force depends on the relative velocity (v_r) between the tool and the workpiece (chip) which is expressed as

$$v_r = v_c - \dot{x}(t), \quad v_c = d/\tau \tag{5}$$

where v_c means the cutting speed which also depends on the time delay τ and a workpiece or a tool diameter d . The coefficients a_r and b_r are responsible for the friction force characteristic presented in Fig. 2. The shape of this characteristic is consistent with the experimental results reported

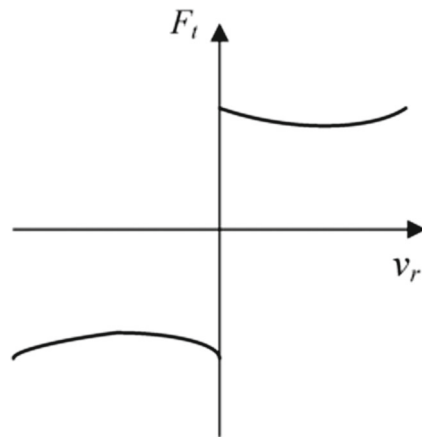


Fig. 2 Friction force characteristic

in [25–29]. The relative velocity v_r can be positive and negative. Therefore, the friction force characteristic has two branches.

3 Analytical solution of chatter vibrations

The non-dimensional equation of motion of the cutting tool (3) is solved analytically by the multiple scale method [30]. At the beginning, it is assumed that the relative velocity (v_r) is still positive and equals 1. Next, two scales—the fast T_0 and the slow T_1 are introduced and defined as follows:

$$T_0 = t, T_1 = \varepsilon t \tag{6}$$

Then, a solution in the first-order approximation has the form:

$$\begin{aligned} x(t) &= x_0(T_0, T_1) + \varepsilon x_1(T_0, T_1) \\ x(t - \tau) &= x_\tau = x_{0\tau}(T_0, T_1) + \varepsilon x_{1\tau}(T_0, T_1) \end{aligned} \tag{7}$$

It is assumed that:

$$\omega_0^2 = \omega^2 + \varepsilon\sigma, \delta = \varepsilon\hat{\delta}, \gamma = \varepsilon\hat{\gamma}, \alpha = \varepsilon\hat{\alpha}, \beta = \varepsilon\hat{\beta} \tag{8}$$

where ε is a formal small parameter. Next, in order to facilitate notation, the tilde is omitted. Using the chain rule, the time derivative is transformed according to the expressions:

$$\begin{aligned} \frac{d}{dt} &= \frac{\partial}{\partial T_0} + \varepsilon \frac{\partial}{\partial T_1} \\ \frac{d^2}{dt^2} &= \frac{\partial^2}{\partial T_0^2} + \varepsilon \frac{\partial^2}{\partial T_0 \partial T_1} + \varepsilon \frac{\partial^2}{\partial T_1 \partial T_0} + \dots \\ &= \frac{\partial^2}{\partial T_0^2} + 2\varepsilon \frac{\partial^2}{\partial T_0 \partial T_1} + \dots \end{aligned} \tag{9}$$

Substituting Eqs. 6–9 into Eq. 3 we get:

$$\begin{aligned} \frac{\partial^2 x(t)}{\partial T_0^2} + 2\varepsilon \frac{\partial^2 x(t)}{\partial T_0 \partial T_1} + \varepsilon \beta b_r \left(\frac{\partial x(t)}{\partial T_0} + \varepsilon \frac{\partial x(t)}{\partial T_1} \right)^3 \\ - 3\varepsilon \beta b_r v_c \left(\frac{\partial x(t)}{\partial T_0} + \varepsilon \frac{\partial x(t)}{\partial T_1} \right)^2 \\ + \varepsilon \left(3\beta b_r v_c^2 - \beta a_r + \delta \right) \left(\frac{\partial x(t)}{\partial T_0} + \varepsilon \frac{\partial x(t)}{\partial T_1} \right) \\ + \varepsilon \alpha \left(\mu x(t) - x_\tau(t) - h_0 \right) + \varepsilon \gamma x(t)^3 \\ + \varepsilon \sigma x(t) + \omega^2 x(t) + \varepsilon \beta \left(a_r v_c - b_r v_c^3 - t_h - c \right) = 0 \end{aligned} \tag{10}$$

For clarity, some part of the mathematical derivations is put in the appendix. Finally, we obtain the modulation equations in the form

$$\begin{aligned} f_1 = a'(T_1) &= -\frac{1}{2}\delta a(T_1) - \frac{1}{2}\alpha a(T_1) \sin \tau \\ &+ \frac{1}{2}\beta a_r a(T_1) - \frac{3}{8}\beta b_r a(T_1)^3 - \frac{3}{2}\beta b_r v_c^2 a(T_1) \\ f_2 = \beta'(T_1) &= \frac{1}{2}\mu \alpha + \frac{1}{2}\sigma + \frac{3}{8}\gamma a(T_1)^2 - \frac{1}{2}\alpha \cos \tau \end{aligned} \tag{11}$$

Then, for the steady-state solution, Eq. 11 take the form:

$$\begin{aligned} -\frac{1}{2}\delta a - \frac{1}{2}\alpha a \sin \tau + \frac{1}{2}\beta a_r a - \frac{3}{8}\beta b_r a^3 - \frac{3}{2}\beta b_r v_c^2 a = 0 \\ \frac{1}{2}\mu \alpha + \frac{1}{2}(\omega_0^2 - \omega^2) + \frac{3}{8}\gamma a^2 - \frac{1}{2}\alpha \cos \tau = 0 \end{aligned} \tag{12}$$

Solving Eq. 12, one trivial (a_1) and two non-trivial (periodic) solutions (a_2) are found.

$$\begin{aligned} a_1 &= 0 \\ a_{2,3} &= 2\sqrt{\frac{a_r - \frac{\delta}{\beta}}{3b_r} \mp \frac{\alpha \sin(\tau)}{3\beta b_r} - \frac{d^2}{\tau^2}} \end{aligned} \tag{13}$$

The trivial solution (a_1) is important from a practical point of view because here the cutting process is stable without chatter vibrations. When the trivial solution is unstable, chatter appears. Therefore, the problem of solution stability is of great importance.

To analyse the stability of steady-state solutions, Eq. 11 are linearised with respect to $a(T_1)$ and $\beta(T_1)$. Next, the Jacobian matrix is defined as

$$J = \begin{pmatrix} \frac{df_1}{da} & \frac{df_1}{d\beta(T_1)} \\ \frac{df_2}{da} & \frac{df_2}{d\beta(T_1)} \end{pmatrix} \tag{14}$$

The eigenvalue of the Jacobian (Eq. 14) should have a negative real part in order to produce a stable solution. The

eigenvalue, which defines stability of trivial and non-trivial solution is expressed as

$$\frac{1}{8}(4a_r\beta - 9a^2b_r\beta - 12b_r\beta(d/\tau)^2 - 4\delta - 4\alpha \sin \tau) \quad (15)$$

Trivial solution stability For the trivial solution ($a_1 = 0$), the eigenvalue (Eq. 15) takes the form

$$\beta(a_r - 3b_r(d/\tau)^2) - \delta - \alpha \sin \tau < 0 \quad (16)$$

The stability borders of the trivial solution determine the so-called stability lobe diagram (SLD) which is shown graphically in Fig. 3 assuming the following parameters: $\delta = 0.1$, $\beta = 0.8$, $a_r = 0.5$, $b_r = 0.1$ and $d = 1$. The SLD shows the plane of the parameters $\Omega - \alpha$ where cutting process is stable (the trivial solution is stable). This area is white in the SLD while the colour lobes point to the chatter vibration amplitude.

Inside the lobes, the non-trivial (periodic) solution exists. Its amplitude and the lobe width depend on the friction force factor (β). At $\beta = 0.01$, the chatter region is smaller, but the amplitude is higher approaching even to 30 (Fig. 3a). At stronger friction ($\beta = 0.1$ and especially $\beta = 0.8$), the chatter region is wider and the amplitudes of chatter are significantly smaller. Thus, friction broadens the chatter region but limits the vibration amplitude.

Stability of non-trivial solutions The non-trivial (periodic) solutions ($a_{2,3}$) are stable when the following equation is satisfied

$$\beta(a_r - 3b_r(d/\tau)^2) - \delta + \alpha\left(\frac{1}{2} \mp \frac{3}{2}\right) \sin \tau > 0 \quad (17)$$

The first periodic solution a_2 is stable exactly when the trivial solutions is unstable, but the second non-trivial solution a_3 is stable in the regions where the trivial solutions is stable. Thus, two solutions: trivial a_1 and periodic a_3 , can exist in the same region of the SLD depending on the initial conditions. The same behaviour observed for the nonlinear regenerative model is reported in [31]. Both periodic solutions (a_2 and a_3) are presented in Fig. 4. Interestingly, that in the first-order approximation chatter vibrations do not depend on cubic nonlinearity determined by the γ coefficient. Probably the solution of the second order approximation reveals the influence of γ on the system's dynamics. Similar diagrams with unstable lobes are obtained on the plane $\Omega - \beta$ (Fig. 5). In this case, three variants of the coefficient of regenerative effect (α) are analysed $\alpha = 0.01$, $\alpha = 0.1$ and $\alpha = 0.4$. For $\alpha = 0.01$ (Fig. 5a) there is a critical value of $\beta = 0.2$. This critical β means that, below this value, the cutting process is free of chatter regardless of ω . Unstable lobes are hardly visible because the whole region $\beta > 0.2$ is unstable. In other words, the

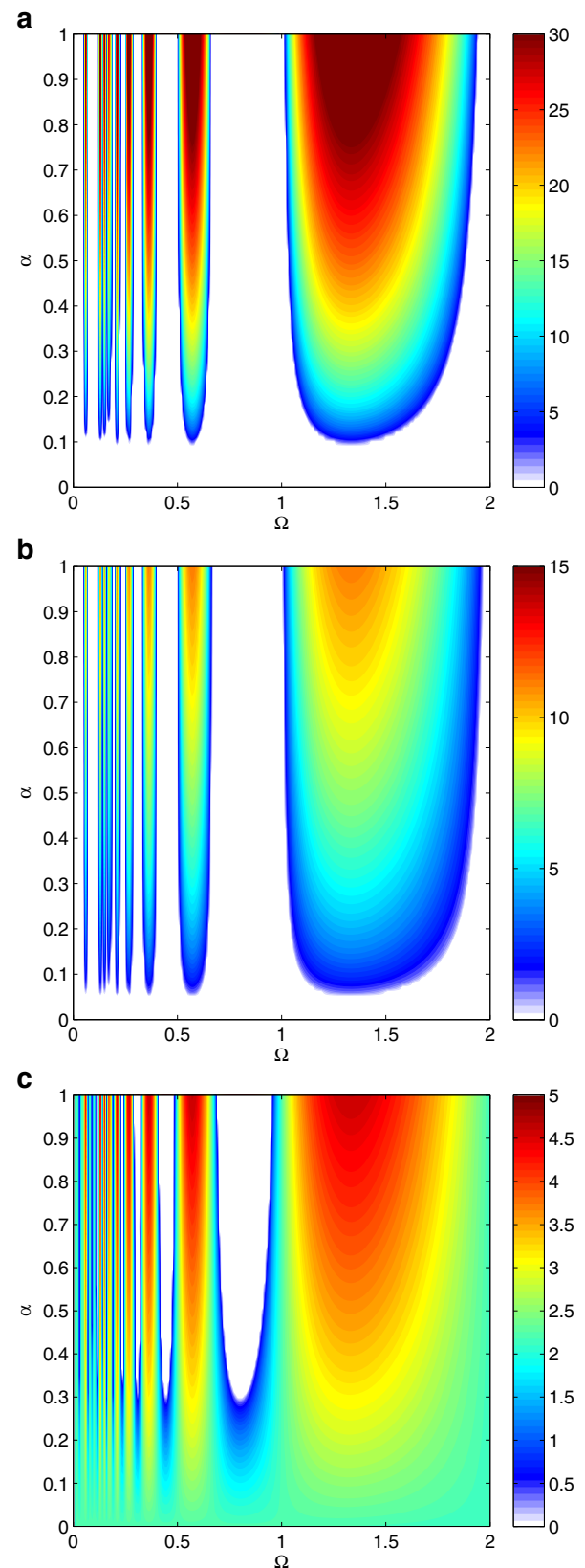


Fig. 3 Stability lobe diagrams. Influence of regeneration mechanism (β) on stability of trivial solution for $\beta = 0.01$ (a), $\beta = 0.1$ (b) and $\beta = 0.8$ (c)

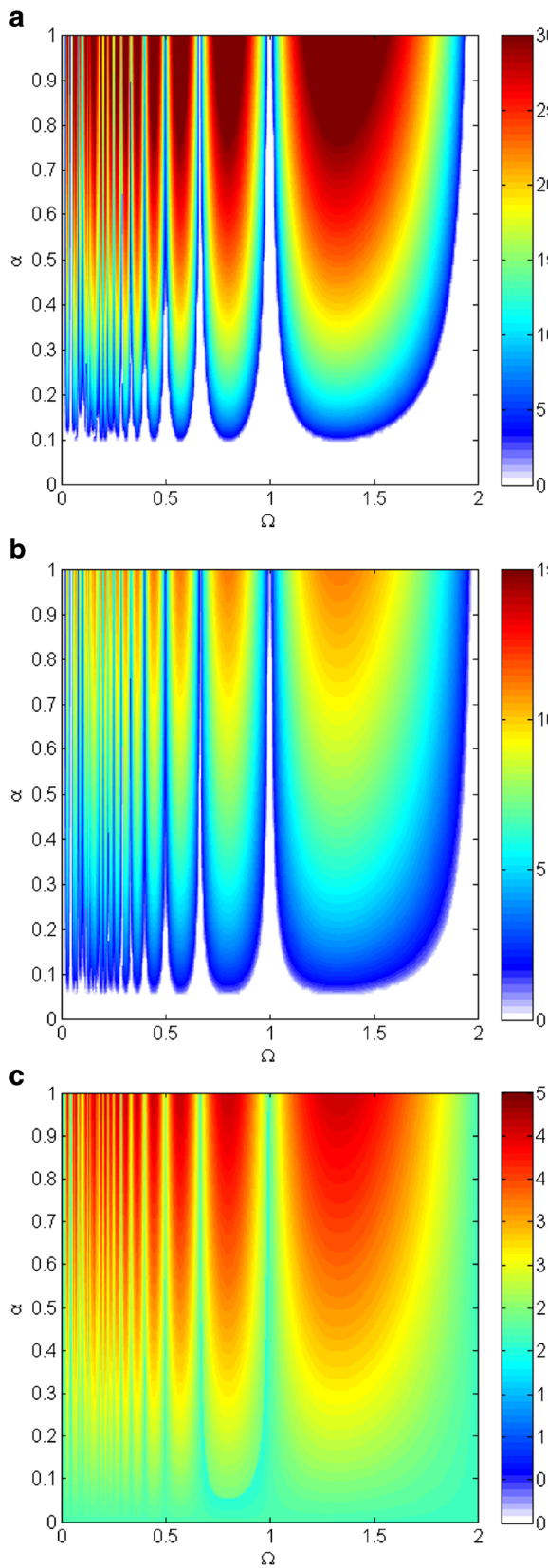


Fig. 4 Stability lobe diagrams. Influence of regeneration mechanism (β) on stability of non-trivial solution for $\beta = 0.01$ (a), $\beta = 0.1$ (b) and $\beta = 0.8$ (c)

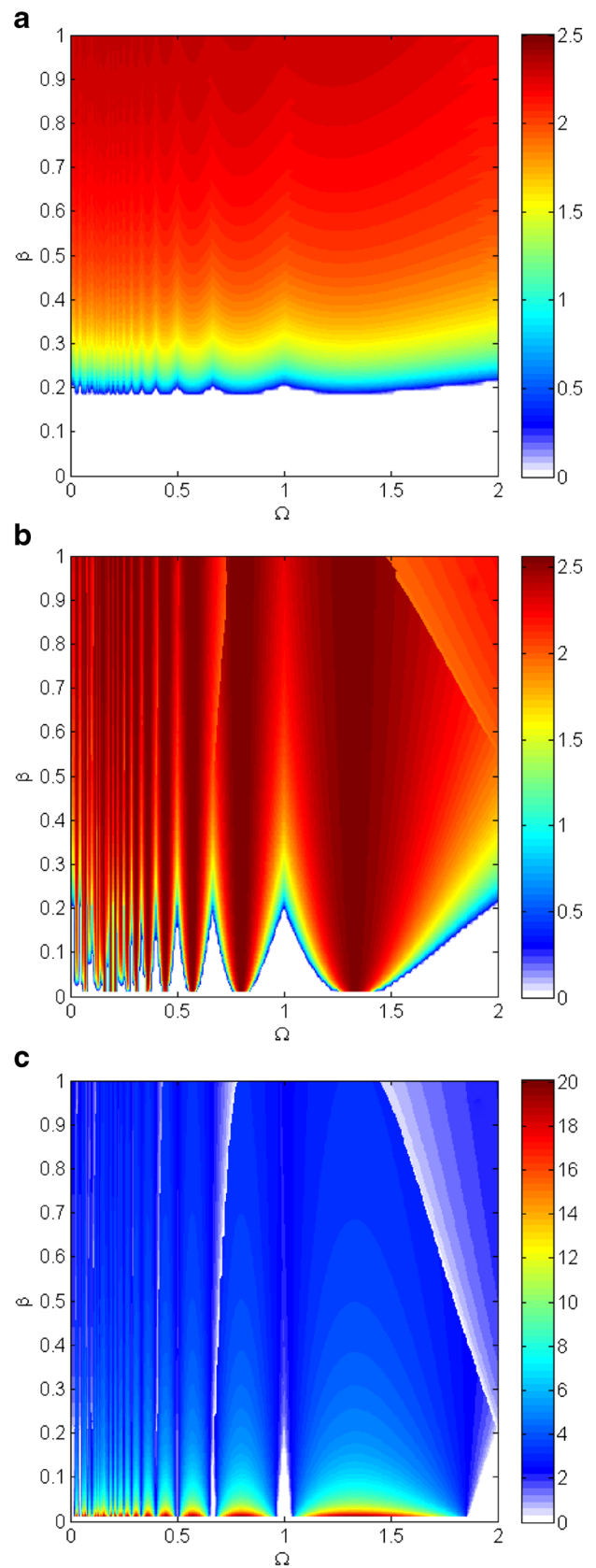


Fig. 5 Influence of friction (β) on stability of non-trivial solution for $\alpha = 0.01$ (a), $\alpha = 0.1$ (b) and $\alpha = 0.4$ (c)

periodic solutions are stable. Unstable lobes are more visible when $\alpha = 0.1$ (Fig. 5b). In the analysed system, the most interesting behaviour can be observed for $\alpha = 0.4$ (Fig. 5c). The highest amplitudes occur for the small β and unstable lobes seem to be inverted. Here, the regenerative mechanism dominates over the frictional one.

4 Discussion and conclusions

Chatter vibrations as a result of classical regenerative and extra frictional mechanisms are investigated here with respect to interactions between them. The analytical method of multiple time scales is used successfully to solve the nonlinear problem of the cutting process. Although the nonlinear properties of the tool stiffness are assumed, their influence on cutting dynamics is not allowed for in the first-order approximation. Probably, the second order approximation would be better to this aim; however, the influence of the frictional mechanism on regenerative chatter is visible. Classical unstable lobes generated by the regenerative effect are modified by the action of friction. The friction phenomenon widens unstable cutting regions, but on the other hand, it reduces the chatter vibration amplitude. The regenerative model of cutting with friction has trivial and two periodic (non-trivial) solutions. The periodic and trivial solutions can exist simultaneously at specific cutting speeds because both solutions can be stable. From practical point of view it means that any disturbance causing a change of initial conditions can lead to chatter even in the region where the classical regenerative cutting process should be stable, this is, for a small α . Such a change of initial conditions can be caused for example by chip break. The interesting phenomenon of reverse unstable lobes is shown on the plane of rotational speed-friction force coefficient ($\Omega - \beta$). We can observe an untypical behaviour where the small β generates a higher vibration amplitude than large one. The stability diagram on the plane of rotational speed (ω)-friction force component (β) is an equivalent of the classical stability lobe diagram (SLD) and can be called a frictional stability lobe diagram—FSLD.

Investigation of friction and regenerative chatter will be continued using the numerical method in order to find aperiodic and irregular vibrations in the nonlinear model of the cutting process. Moreover, experimental tests are planned to be performed in order to verify the theoretical results, and most of all, to obtain the real coefficient of frictional and regenerative force components.

Acknowledgments The work of the first author is financially supported by the National Science Centre under the project no. DEC-2013/09/N/ST8/01202. The contribution of the second author is financially supported by the National Science Centre under the project no. DEC-2011/01/B/ST8/07504.

Open Access This article is distributed under the terms of the Creative Commons Attribution 4.0 International License (<http://creativecommons.org/licenses/by/4.0/>), which permits unrestricted use, distribution, and reproduction in any medium, provided you give appropriate credit to the original author(s) and the source, provide a link to the Creative Commons license, and indicate if changes were made.

Appendix

Expanding derivatives of the Eq. 10, we obtain:

$$\begin{aligned}\frac{\partial x(t)}{\partial T_0} &= \frac{\partial x_0}{\partial T_0} + \varepsilon \frac{\partial x_1}{\partial T_0} \\ \frac{\partial^2 x(t)}{\partial T_0^2} &= \frac{\partial^2 x_0}{\partial T_0^2} + \varepsilon \frac{\partial^2 x_1}{\partial T_0^2} \frac{\partial^2 x(t)}{\partial T_0 \partial T_1} \\ &= \frac{\partial^2 x_0}{\partial T_0 \partial T_1} + \varepsilon \frac{\partial^2 x_1}{\partial T_0 \partial T_1}\end{aligned}\quad (18)$$

$$\begin{aligned}\varepsilon \frac{\partial^2 x_1}{\partial T_0^2} + \frac{\partial^2 x_0}{\partial T_0^2} + 2\varepsilon \frac{\partial^2 x_0}{\partial T_0 \partial T_1} + \varepsilon \beta b_r \left(\frac{\partial x_0}{\partial T_0} \right)^3 \\ - 3\varepsilon \beta b_r v_c \left(\frac{\partial x_0}{\partial T_0} \right)^2 + \varepsilon \left(3\beta b_r v_c^2 - \beta a_r + \delta \right) \left(\frac{\partial x_0}{\partial T_0} \right) \\ + \varepsilon \alpha (\mu x_0 - x_{0\tau} - h_0) + \varepsilon \gamma x_0^3 \\ + \varepsilon \sigma x_0 + \omega^2 x_0 + \varepsilon \omega^2 x_1 \\ + \varepsilon \beta (a_r v_c - b_r v_c^3 - t_h - c) = 0\end{aligned}\quad (19)$$

Equating coefficients of powers of ε^0 and ε^1 , we obtain:

$$\begin{aligned}\varepsilon^0 \Rightarrow \frac{\partial^2 x_0}{\partial T_0^2} + \omega^2 x_0 = 0 \\ \varepsilon^1 \Rightarrow \frac{\partial^2 x_1}{\partial T_0^2} + 2 \frac{\partial^2 x_0}{\partial T_0 \partial T_1} + \beta b_r \left(\frac{\partial x_0}{\partial T_0} \right)^3 \\ - 3\beta b_r v_c \left(\frac{\partial x_0}{\partial T_0} \right)^2 + \left(3\beta b_r v_c^2 - \beta a_r + \delta \right) \left(\frac{\partial x_0}{\partial T_0} \right) \\ + \alpha (\mu x_0 - x_{0\tau} - h_0) + \gamma x_0^3 + \omega^2 x_1 \\ + \sigma x_0 + \beta (a_r v_c - b_r v_c^3 - t_h - c) = 0\end{aligned}\quad (20)$$

It is convenient to express the solution of first Eq. 20 in the complex form:

$$\begin{aligned}x_0(T_0, T_1) &= A(T_1)e^{iT_0} + \bar{A}(T_1)e^{-iT_0} \\ x_{0\tau}(T_0, T_1) &= A(T_1)e^{i(T_0-\tau)} + \bar{A}(T_1)e^{-i(T_0-\tau)}\end{aligned}\quad (21)$$

where \bar{A} is the complex conjugate of A , which is an arbitrary complex function of T_1 . Substituting Eq. 21 into second Eq. 20 and expanding the derivatives, we get:

$$\begin{aligned}\frac{\partial x_0}{\partial T_0} &= A(T_1)ie^{iT_0} - \bar{A}(T_1)ie^{-iT_0} \\ \frac{\partial^2 x_0}{\partial T_0 \partial T_1} &= A'(T_1)ie^{iT_0} - \bar{A}'(T_1)ie^{-iT_0}\end{aligned}\quad (22)$$

and then the following equation is obtained:

$$\begin{aligned} & \frac{\partial^2 x_1}{\partial T_0^2} + \omega^2 x_1 + 2 \left(A'(T_1) i e^{iT_0} - \bar{A}'(T_1) i e^{-iT_0} \right) \\ & + \beta b_r \left(A(T_1) i e^{iT_0} - \bar{A}(T_1) i e^{-iT_0} \right)^3 \\ & - 3\beta b_r v_c \left(A(T_1) i e^{iT_0} - \bar{A}(T_1) i e^{-iT_0} \right)^2 \\ & + \left(3\beta b_r v_c^2 - \beta a_r + \delta \right) \left(A(T_1) i e^{iT_0} - \bar{A}(T_1) i e^{-iT_0} \right) \\ & + \alpha \mu \left[A(T_1) e^{iT_0} + \bar{A}(T_1) e^{-iT_0} \right] \\ & - \alpha \left[A(T_1) e^{i(T_0-\tau)} + \bar{A}(T_1) e^{-i(T_0-\tau)} \right] - \alpha h_0 \\ & + \gamma \left(A(T_1) e^{iT_0} + \bar{A}(T_1) e^{-iT_0} \right)^3 \\ & + \sigma \left(A(T_1) e^{iT_0} + \bar{A}(T_1) e^{-iT_0} \right) \\ & + \beta \left(a_r v_c - b_r v_c^3 - t_h - c \right) = 0 \end{aligned} \tag{23}$$

Ordering Eq. 23, we get its final form

$$\begin{aligned} & \frac{\partial^2 x_1}{\partial T_0^2} + \omega^2 x_1 + (i\delta A(T_1) + \alpha \mu A(T_1) \\ & + \sigma A(T_1) - i\beta a_r A(T_1) + 3i\beta b_r v_c^2 A(T_1) \\ & + 3\gamma A(T_1)^2 \bar{A}(T_1) \\ & + 3i\beta b_r A(T_1)^2 \bar{A}(T_1) + 2i A'(T_1) - \alpha A(T_1) e^{-i\tau}) e^{iT_0} \\ & + (-i\delta \bar{A}(T_1) + \alpha \mu \bar{A}(T_1) \\ & + \sigma \bar{A}(T_1) + i\beta a_r \bar{A}(T_1) - 3i\beta b_r v_c^2 \bar{A}(T_1) \\ & + 3\gamma \bar{A}(T_1)^2 A(T_1) - 3i\beta b_r \bar{A}(T_1)^2 A(T_1) \\ & - 2i \bar{A}'(T_1) - \alpha \bar{A}(T_1) e^{-i\tau}) e^{-iT_0} \\ & + 3\beta b_r v_c A(T_1)^2 e^{2iT_0} + 3\beta b_r v_c \bar{A}(T_1)^2 e^{-2iT_0} \\ & + (\gamma - i\beta b_r) A(T_1)^3 e^{3iT_0} + (\gamma + i\beta b_r) \bar{A}(T_1)^3 e^{-3iT_0} \\ & - 6\beta b_r v_c A(T_1) \bar{A}(T_1) \\ & + \beta \left(a_r v_c - b_r v_c^3 - t_h - c \right) - \alpha h_0 = 0 \end{aligned} \tag{24}$$

The secular term of Eq. 24 vanishes if and only if:

$$ST_1 e^{iT_0} = 0, \quad ST_2 e^{-iT_0} = 0 \tag{25}$$

where ST_1 and ST_2 are the secular generating terms. This leads to the equations:

$$\begin{aligned} & i\delta A(T_1) + \alpha \mu A(T_1) + \sigma A(T_1) - i\beta a_r A(T_1) \\ & + 3i\beta b_r v_c^2 A(T_1) + 3\gamma A(T_1)^2 \bar{A}(T_1) \\ & + 3i\beta b_r A(T_1)^2 \bar{A}(T_1) + 2i A'(T_1) - \alpha A(T_1) e^{-i\tau} = 0 \\ & -i\delta \bar{A}(T_1) + \alpha \mu \bar{A}(T_1) + \sigma \bar{A}(T_1) + i\beta a_r \bar{A}(T_1) \\ & - 3i\beta b_r v_c^2 \bar{A}(T_1) + 3\gamma \bar{A}(T_1)^2 A(T_1) \\ & - 3i\beta b_r \bar{A}(T_1)^2 A(T_1) - 2i \bar{A}'(T_1) - \alpha \bar{A}(T_1) e^{-i\tau} = 0 \end{aligned} \tag{26}$$

Substituting into Eq. 26, the polar form of the complex amplitude:

$$\begin{aligned} A(T_1) &= \frac{1}{2} a(T_1) e^{i\beta(T_1)} \\ A'(T_1) &= \frac{1}{2} a'(T_1) e^{i\beta(T_1)} + \frac{1}{2} i a(T_1) \beta'(T_1) e^{i\beta(T_1)} \\ \bar{A}(T_1) &= \frac{1}{2} a(T_1) e^{-i\beta(T_1)} \\ \bar{A}'(T_1) &= \frac{1}{2} a'(T_1) e^{-i\beta(T_1)} - \frac{1}{2} i a(T_1) \beta'(T_1) e^{-i\beta(T_1)} \end{aligned} \tag{27}$$

results in:

$$\begin{aligned} & -\frac{1}{2} \alpha a(T_1) e^{-i\tau + i\beta(T_1)} + \frac{1}{2} i \delta a(T_1) e^{i\beta(T_1)} \\ & + \frac{1}{2} \mu \alpha a(T_1) e^{i\beta(T_1)} + \frac{1}{2} \sigma a(T_1) e^{i\beta(T_1)} \\ & + \frac{3}{8} \gamma a(T_1)^3 e^{i\beta(T_1)} - \frac{1}{2} i \beta a_r a(T_1) e^{i\beta(T_1)} \\ & + \frac{3}{8} i \beta b_r a(T_1)^3 e^{i\beta(T_1)} + \frac{3}{2} i \beta b_r v_c^2 a(T_1) e^{i\beta(T_1)} \\ & + 2i \left[\frac{1}{2} a'(T_1) e^{i\beta(T_1)} + \frac{1}{2} i a(T_1) \beta'(T_1) e^{i\beta(T_1)} \right] = 0 \\ & -\frac{1}{2} \alpha a(T_1) e^{i\tau - i\beta(T_1)} - \frac{1}{2} i \delta a(T_1) e^{-i\beta(T_1)} \\ & + \frac{1}{2} \mu \alpha a(T_1) e^{-i\beta(T_1)} + \frac{1}{2} \sigma a(T_1) e^{-i\beta(T_1)} \\ & + \frac{3}{8} \gamma a(T_1)^3 e^{-i\beta(T_1)} \\ & + \frac{1}{2} i \beta a_r a(T_1) e^{-i\beta(T_1)} \\ & - \frac{3}{8} i \beta b_r a(T_1)^3 e^{-i\beta(T_1)} \\ & - \frac{3}{2} i \beta b_r v_c^2 a(T_1) e^{-i\beta(T_1)} \\ & - 2i \left[\frac{1}{2} a'(T_1) e^{-i\beta(T_1)} - \frac{1}{2} i a(T_1) \beta'(T_1) e^{-i\beta(T_1)} \right] = 0 \end{aligned} \tag{28}$$

After the transformations of the first Eq. 28, we obtain:

$$\begin{aligned} & -\frac{1}{2} \alpha a(T_1) e^{-i\tau} + \frac{1}{2} i \delta a(T_1) + \frac{1}{2} \mu \alpha a(T_1) \\ & + \frac{1}{2} \sigma a(T_1) + \frac{3}{8} \gamma a(T_1)^3 - \frac{1}{2} i \beta a_r a(T_1) \\ & + \frac{3}{8} i \beta b_r a(T_1)^3 + \frac{3}{2} i \beta b_r v_c^2 a(T_1) + i a'(T_1) \\ & - a(T_1) \beta'(T_1) = 0 \end{aligned} \tag{29}$$

Then recalling

$$e^{-i\tau} = \cos \tau - i \sin \tau \tag{30}$$

The normal form is obtained:

$$\begin{aligned} & \frac{1}{2}i\delta a(T_1) + \frac{1}{2}\mu\alpha a(T_1) + \frac{1}{2}\sigma a(T_1) + \frac{3}{8}\gamma a(T_1)^3 \\ & - \frac{1}{2}\alpha a(T_1) \cos \tau + \frac{1}{2}i\alpha a(T_1) \sin \tau \\ & - \frac{1}{2}i\beta a_r a(T_1) + \frac{3}{8}i\beta b_r a(T_1)^3 + \frac{3}{2}i\beta b_r v_c^2 a(T_1) \\ & + ia'(T_1) - a(T_1)\beta'(T_1) = 0 \end{aligned} \quad (31)$$

Separating the real and imaginary parts, the two, so-called, modulation equations are found:

$$\begin{aligned} & \frac{1}{2}\delta a(T_1) + \frac{1}{2}\alpha a(T_1) \sin \tau - \frac{1}{2}\beta a_r a(T_1) \\ & + \frac{3}{8}\beta b_r a(T_1)^3 + \frac{3}{2}\beta b_r v_c^2 a(T_1) + a'(T_1) = 0 \\ & \frac{1}{2}\mu\alpha a(T_1) + \frac{1}{2}\sigma a(T_1) + \frac{3}{8}\gamma a(T_1)^3 \\ & - \frac{1}{2}\alpha a(T_1) \cos \tau - a(T_1)\beta'(T_1) = 0 \end{aligned} \quad (32)$$

References

- Taylor F (1907) On the art of cutting metal. *Trans ASME* 28:31–248
- Thusty J, Polacek M (eds) (1963) Stability of machine tools against self-excited vibration in machining. *Proc ASME Prod Eng Res Conf*
- Tobias SA (1965) Machine tool vibration. John Wiley, New York and USA
- Kudinov VA (1955) Theory of vibration generated from metal cutting. *New Technology of Mechanical Engineering*:1–7
- Kudinov VA (1963) Dynamics characteristics of the metal cutting process. *Stanki i Instrument* 10:1–7
- Grabec I (1986) Chaos generated by the cutting process. *Phys Lett A* A117:384–386
- Grabec I (1998) Chaotic dynamics of the cutting process. *Int J Mach Tools Manuf* 28(1):19–32
- Lipski J, Litak G, Rusinek R, Szabelski K, Teter A, Warminski J, Zaleski K (2002) Surface quality of a work material's influence on the vibrations of the cutting process. *J Sound Vib* 252(4):739–737
- Rusinek R, Wiercigroch M, Wahi P (2014) Influence of tool flank forces on complex dynamics of cutting process. *Int J Bifurcation Chaos* 24(09):1450115
- Rusinek R, Wiercigroch M, Wahi P (2014) Modelling of frictional chatter in metal cutting. *Int J Mech Sci* 89:167–176
- Wiercigroch M (1997) Chaotic vibration of a simple model of the machine tool-cutting process system. *J Vib Acoust* 119:468–475
- Wiercigroch M, Budak E (2001) Sources of nonlinearities, chatter generation and suppression in metal cutting. *Philos Trans R Soc A Math Phys Eng Sci* 359(1781):663–693
- Wiercigroch M, Krivtsov AM (2001) Frictional chatter in orthogonal metal cutting. *Phil Trans The Royal Society of London A Mathematical Physical And Engineering Science* 359:713–738
- Rusinek R, Kecik K, Warminski J, Weremczuk A (2011) Dynamic model of cutting process with modulated spindle speed. *AIP Conf Proc*:805–809
- Gradisek J, Grabec I, Siegert S, Friedrich R (2002) Stochastic dynamics of metal cutting: bifurcation phenomena in turning. *Mech Syst Signal Process* 16(5):831–840
- Kalmar-Nagy T, Wahi P (2008) Towards practical stability limits in Turning. In: *Proceedings of the 6th EUROMECH Nonlinear Oscillations Conference* St. Petersburg, Russia
- Stepan G (2001) Modelling nonlinear regenerative effect in metal cutting. *Philos Trans R Soc A Math Phys Eng Sci* 359:739–757
- Stepan G, Szalai R, Insperger T (2004) Nonlinear dynamics of high-speed milling subjected to regenerative effect. In: Radons G, Neugebauer R (eds) *Nonlinear Dynamics of Production Systems* 111–127. Wiley-VCH, Weinheim
- Nayfeh AH, Chin CM, Pratt J (1997) Perturbation methods in nonlinear dynamics-applications to machining dynamics. *J Manuf Sci Eng* 119:485–493
- Wan M, Ma YC, Feng J, Zhang WH (2016) Study of static and dynamic ploughing mechanisms by establishing generalized model with static milling forces. *Int J Mech Sci* 114:120–131
- Wan M, Murat Kilic Z, Altintas Y (2015) Mechanics and dynamics of multifunctional tools. *J Manuf Sci Eng* 137(1):011019
- Wan M, Altintas Y (2014) Mechanics and dynamics of thread milling process. *Int J Mach Tools Manuf* 87:16–26
- Wan M, Ma YC, Zhang WH, Yang Y (2015) Study on the construction mechanism of stability lobes in milling process with multiple modes. *Int J Adv Manuf Technol* 79(1-4):589–603
- Lin JS, Weng CI (1991) Nonlinear dynamics of cutting process. *Int J Mech Sci* 33(8):645
- Zemzemi F, Rech J, Ben Salem W, Dogui A, Kapsa P (2009) Identification of a friction model at tool/chip/workpiece interfaces in dry machining of aISI4142 treated steels. *J Mater Process Technol* 209(8):3978–3990
- Rech J, Claudin C, D'Eramo E (2009) Identification of a friction model—application to the context of dry cutting of an AISI 1045 annealed steel with a TiN-coated carbide tool. *Tribol Int* 42(5):738–744
- Childs THC (2006) Friction modelling in metal cutting. *Tribology in Manufacturing Processes* 260(3):310–318
- Stembalski M, Preś P, Skoczyński W (2013) Determination of the friction coefficient as a function of sliding speed and normal pressure for steel c45 and steel 40HM. *Archives of Civil and Mechanical Engineering* 13(4):444–448
- San-Juan M, Martín Ó, Santos F (2010) Experimental study of friction from cutting forces in orthogonal milling. *Int J Mach Tools Manuf* 50(7):591–600
- Nayfeh AH (1985) Problems in perturbation. John Wiley & Sons, Inc
- Rusinek R, Weremczuk A, Warminski J (2011) Regenerative model of cutting process with nonlinear Duffing oscillator. *Mechanics and Mechanical Engineering* 15(4):129–143